POLITECNICO DI TORINO
Repository ISTITUZIONALE

Modeling the herd prey response to individualistic predators attacks

(Article begins on next page)

23 April 2024

RESEARCH ARTICLE

WILEY

Modeling the herd prey response to individualistic predators attacks

Francesca Acotto [ID] | **Ezio Venturino** [ID]

Dipartimento di Matematica "Giuseppe Peano", Università di Torino, via Carlo Alberto 10, Turin, 10123, Italy

Correspondence
Ezio Venturino, Dipartimento di Matematica "Giuseppe Peano", Università di Torino, via Carlo Alberto 10, 10123 Turin, Italy.
Email: ezio.venturino@unito.it

Communicated by: R. Bravo de la Parra

In this paper, we consider predators hunting on prey gathered in groups and in such way exhibiting the possibility of reducing the predators pressure. To model this feature, however, we depart from the Holling type II (HTII) response function, in that we assume that a sufficiently large set of prey could respond to individualistic attacks and therefore induce the predator to renounce. The basic idea is described at first in a simple two-populations predator-prey system. It is then expanded considering the generalist predators to deal with two prey. In the first case, both are gathered in herds, and in the second one, one of the two instead behaves individualistically. The net outcome is an enhanced survival for the prey with respect to both the herding cases without and with predators feeding satiation (i.e., using the HTII response).

KEYWORDS
boundary interactions, competition, generalist predators, herd behavior, individualistic attacks, predator-prey, prey response to attacks

MSC CLASSIFICATION
92D25, 92D40, 92D50

1 | INTRODUCTION

In this paper, we introduce a new model for investigating the possible reaction to predators attacks that prey living in herds may exhibit, if they are in large enough numbers. To this end, we use concepts that appeared in the literature, such as [1] and [2], that investigate very similar models, as well as [3] and [4]. In the first pair of papers, the mass action law, corrected with the square root functional response, to account for predation possibly being exercised on the boundary of the herd, describes the predator-prey interactions, while the last two both contain instead HTII terms.

The idea explored in this paper consists in rendering in mathematical terms the observation that if the herding prey are in large numbers, the predators' attacks should indeed decrease, as the prey have a better chance to defend themselves.

Note that a similar consideration in the epidemiology domain has led to the formulation of a now classic model for disease propagation. Namely, the idea is that with a larger number of infected, individuals tend to reduce their contacts in order to escape from contagion [5]. This has also been the basis for the lockdown policies implemented by various governments during the Covid-19 pandemic.

The main results of the paper are shown in and summarized by Figures 5–7, which compare the equilibria of the various above-mentioned models, as function of several system parameters. In all of them, the gathering prey that have suitable population sizes are shown to be better off under predators' attacks than those modeled by other behavioral assumptions.

The paper is organized as follows. The next two sections describe in detail the ecological situation and the main novel idea. Section 4 contains a simple predator-prey with these new features. The next two sections, respectively, describe the predator-two herding prey system and the predator-individualistic prey-herding prey system. A final discussion concludes the paper.

2 | ECOLOGICAL BACKGROUND

Starting from the classical Lotka-Volterra model, over the years, several other increasingly sophisticated and complex models have been built. In particular, different interaction dynamics have been considered, which differ from the classical assumption of biquadratic terms involving prey and predators. Among these of interest is the case of the prey grazing in large groups coexisting on a common ground with their predators. In the savannah environment, herbivores behaving in such a way are, for example, zebras (*Equus quagga*), gazelles (*Gazella dorcas*), and buffaloes (*Syncerus caffer*). Examples of predators feeding on the former are cheetahs (*Acinonyx jubatus*) and leopards (*Panthera pardus*). Living in groups represents indeed one of the strategies that herbivores use to defend themselves from predators attacks. Various other defense mechanisms are used by animals to avoid being spotted and caught by predators, for instance, the production of repellent substances or the use of camouflage colors. The choice to live in herds, in particular, is classified among the behavioral defense mechanisms, favoring signaling the predators presence to other individuals of the same species, to minimize their detection or enabling them to escape [6].

There are several advantages for prey aggregation.

- A predator is less likely to encounter prey gathered in a single group than prey scattered throughout a territory, although a large herd is more easily spotted.
- A single individual in a herd is less likely to be attacked by predators [7].
- A feeding isolated animal is an easy prey, because it lowers the head and loses sight of the surrounding environment. In a group, this is not a problem because at any time, there will always be some individuals that vigilate and warn about possible approaching dangers; thus, mass collaboration enhances a higher surveillance level and allows more time for feeding for the single individuals [8, 9].
- Large predators generally catch a single escaping prey. For instance, the gazelle is able to reach a speed of 80 km/h, but this is outperformed by chasing cheetahs running at 130 km/h. Faced with the fast movements of an entire group of prey, the predator is disoriented and has difficulties in selecting a precise target, with an increase of the disturbance with an increasing size of the herd, the so-called predator confounding effect. This mechanism is exploited by shoals of fish and flocks of birds [10].
- A large herd size, especially in the case of large herbivores such as buffaloes, discourages hunting attempts by predators. In addition, structural elements of passive defense, for example, size and strong horns, contribute to reduce predators attacks [11], as the latter may be struck back and injured.

Thus, not only aggregation is advantageous for animals in terms of defense but also the benefits it brings increase with the size of the herd. In this paper, we address exactly this issue, that larger herd sizes should reduce the predators attacks.

Predators hunting on prey herd is ultimately modeled by observing that the most likely individuals targeted by the attack are those that reside on the perimeter of the flock, which is a one-dimensional manifold, while the prey population N is distributed over a two-dimensional domain. Thus, the size of the possible captured prey should be proportional to the perimeter length; that is, it would be $\approx \sqrt{N}$ [1]. This specific term should then appear in the mathematical formulation for the predator-prey interactions, replacing the N appearing in the classical models. Note that the choice of the square root functional form is specific for simple shapes of the herd, such as squares or circles. Therefore, it does not appear to be much realistic as herds in natural landscapes may have very much different and more complicated forms. On the other hand, it is relatively easy to use. More general forms involving a generic exponent, such as N^γ, $1 > \gamma \geq 1/2$, could be used. However, in [12], it is observed that this change does not lead to qualitatively relevant novel features. Therefore, in this paper, we use the above simpler formulation.

A number of papers have subsequently appeared based on these assumptions, for instance, incorporating the phenomenon of predator satiation, modeled by a Holling type II (HTII) response function [2, 4, 13, 14]. Another line of investigation includes instead the presence of diseases, explored, for instance, in [3, 15, 16]. Interestingly, it is found that herding reduces the advantages due to symbiosis, while enhances coexistence in a competing system, because essentially the interactions among the two populations involve less individuals than in the one-to-one classical systems [17].

Extensions studying the diffusive spatial behavior have been considered in [18–22], which may lead to pattern formation phenomenon.

3 | THE MAIN NOVEL FEATURE

As discussed above, we want to take in consideration here that in some cases, hunting is hindered by larger prey herd sizes. Thus, not only feeding satiation occurs; that is, the predation rate attains in the limit a saturation level even if the prey are abundant, but if the prey are in large numbers, the predators attacks should indeed decrease.

Mathematically, in our setting involving the square root formulation, this change would correspond to replacing the HTII-like functional response

$$\frac{\sqrt{N}}{1 + b\sqrt{N}} \tag{1}$$

that exhibits a horizontal asymptote at b^{-1}, by an ultimately decreasing function of N. Indeed, we need such a decrease because the larger the prey, the smaller the effects of the predators' attacks. Thus, the function used in (1) would need to be modified and have a denominator that increases faster then the numerator, to satisfy this request. The simplest denominator that exhibits such behavior would be linear. Thus, specifically, we take

$$\frac{\sqrt{N}}{1 + bN}. \tag{2}$$

This function behaves like a classical Gamma function, raising up from the origin, to a peak and then decreasing steadily to 0 as N grows large. In a later section, namely, Section 6, when dealing with an individualistic prey, the chosen functional response would be the standard HTII term. The predators are always assumed to have an individualistic hunting behavior, as well as being generalists. This means that they do not just thrive on the prey considered in the system, but have alternative food sources not explicitly modeled but suitably represented mathematically via a logistic term.

In addition to the simple case of one prey gathered in a herd, two different cases involving a system in which the predator possibly feeds on two different prey will be considered. They differ in that one prey always lives in group, the other one may not or may exhibit an individualistic behavior. The models incorporate direct prey intraspecific competition and allow for possible prey interspecific competition for resources, which occurs for instance in sharing the pastures, that is, herbaceous plants or shrubs, and water. In particular, note that interspecific competition among prey concerns resources distributed across the territory and therefore has nothing to do with the previous assumptions on the role of the herd perimeter. Indeed, a meadow would be grazed by the whole herd, and such action subtracts feeding to the whole other prey population. Thus, the interspecific competition terms involve the whole prey populations N and M and are therefore mathematically represented by the usual biquadratic forms NM. The same consideration applies and justifies the use of the quadratic terms for intraspecific competition, for each prey population, contained in the logistic terms.

4 | THE BASIC MODEL: PREDATOR AND PREY IN A HERD

To illustrate the ideas that we introduce in this paper, we start from a simple predator-prey model composed of predators, behaving individualistically, and a herd of prey. The difference in the prey behavior that we want to explore here consists in the fact that it has the ability of responding to the predators attacks. This occurs when the size of the herd is large enough.

The herd behavior is in general represented by a power function [12], which here we take to be the square root [1], modified so that the predators feeding satiation phenomenon is accounted for. Typically, this is modeled by the classical Holling-type II response function. For the herd behavior, this would involve the presence of a square root term both in the numerator and in the denominator. Here, however, we assume that a large population of prey of reasonable individual size, for example, buffalos or bulls, has the possibility of reacting to the attacks of single predators. To model this effect, we then modify the denominator, so that for large prey populations, this term tends to vanish.

Let N and P, respectively, represent the prey and generalist predator populations. The model we propose reads as follows:

$$\frac{dN}{dt} = rN\left(1 - \frac{N}{K}\right) - \frac{a\sqrt{N}P}{1 + bN} \tag{3}$$

$$\frac{dP}{dt} = sP\left(1 - \frac{P}{H}\right) + \frac{ea\sqrt{N}P}{1 + bN}. \tag{4}$$

TABLE 1 Parameter description.

Parameters	Description	Dimensions
a	hunting rate	$\frac{1}{[t]}$
b	product of handling time and hunting rate	-
e	conversion coefficient	-
r	prey reproduction rate	$\frac{1}{[t]}$
s	predators reproduction rate	$\frac{1}{[t]}$
K	prey carrying capacity	-
H	predators carrying capacity	-

All the parameters are assumed to be nonnegative. They are listed in Table 1. Note that the individualistic behavior of the predators is represented by the classical exponent 1 for P in the numerator of the interaction terms. It is assumed that the prey grow logistically with reproduction rate r and carrying capacity K, and similarly occurs for the predators, being generalist, with growth rate s and carrying capacity H, due to available resources that are not explicitly modeled. The remaining parameters denote the predators attack rate a, the product of handling time and hunting rate b, and the conversion coefficient e.

4.1 | Analysis of the equilibria

Three of the equilibria of the model (3)–(4) are easily determined, namely, $E_0 = (0, 0)$, $E_P = (0, H)$ and $E_N = (K, 0)$, which are all unconditionally feasible. Coexistence is discussed in Appendix A.1.1.

For stability assessment, we need the Jacobian J of the system (3) and (4):

$$
J = \begin{bmatrix} r - \dfrac{2rN}{K} - \dfrac{aP}{2\sqrt{N}(1+bN)} + \dfrac{ab\sqrt{N}P}{(1+bN)^2} & -\dfrac{a\sqrt{N}}{1+bN} \\[2ex] \dfrac{aeP}{2\sqrt{N}(1+bN)} - \dfrac{abe\sqrt{N}P}{(1+bN)^2} & s - \dfrac{2sP}{H} + \dfrac{ae\sqrt{N}}{1+bN} \end{bmatrix}.
$$

Clearly, for $N = 0$, there appears a singularity in some terms of the first column of J. But in this case, the prey vanish, and the predators' equation (4) in such case shows that they attain the carrying capacity H, drifting away from $P = 0$, thereby indicating that the origin E_0 is unstable. The other possible system equilibria lying on the vertical axis, $N = 0$, $(0, H)$, is also unstable. Indeed, setting $\eta = N$ and $\zeta = P - H$, we obtain from the linearization of Equations (3) and (4)

$$
\frac{d\eta}{dt} \approx \sqrt{\eta}\left[r\sqrt{\eta} - \frac{aH}{1+b\eta} \right] \approx -\sqrt{\eta}\, aH < 0
$$

for η small. On the other hand, we have

$$
\frac{d\zeta}{dt} \approx (H + \zeta)\left[\frac{ae\sqrt{\eta}}{1+b\eta} - s\frac{\zeta}{H} \right].
$$

The latter expression is positive for both η and ζ small, if $ae\sqrt{\eta} > s\zeta H^{-1}$, so that with this restriction on the rates at which the populations tend to E_P, the predators population drifts away from H. Consequently, the equilibrium E_P thus turns out to be unconditionally unstable.

The analysis for E_N is simpler, as the Jacobian evaluated at this point is triangular, and its eigenvalues are

$$
-r, \quad s + \frac{ae\sqrt{K}}{1+bK} > 0,
$$

so that it is also unconditionally unstable.

Appendix A.1.2 contains the details of the stability for the coexistence equilibrium.

The fact that both feasibility and stability conditions of this coexistence equilibrium are simultaneously satisfied is shown through numerical simulations, shown in Figure 1.

Table 2 summarizes the stability conditions of all the equilibria.
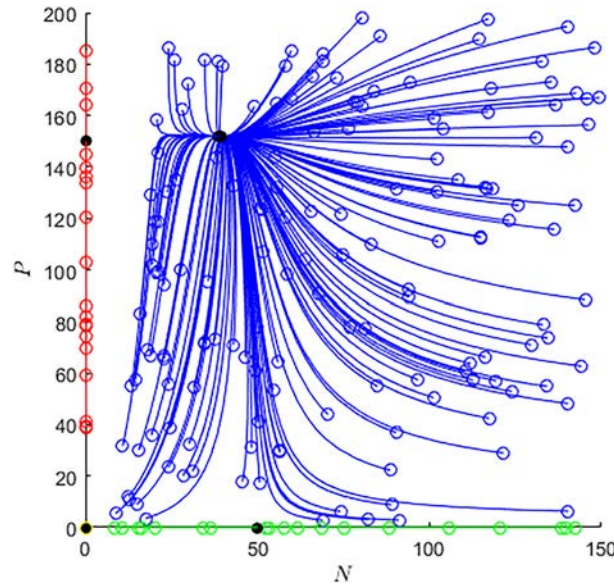
FIGURE 1 Coexistence equilibrium obtained for the parameters $a = 0.2$, $b = 0.8$, $e = 0.3$, $r = 0.7$, $s = 0.9$, $H = 150$, $K = 50$. The initial conditions (empty circles) are randomly chosen in the interior of the first quadrant, and trajectories approach the point E_{NP}. For the initial conditions on the coordinate axis, the trajectories approach the points E_N and E_P, the black dots on the axes, but in the phase plane, these points are unstable. The origin is instead unconditionally unstable. [Colour figure can be viewed at wileyonlinelibrary.com]

TABLE 2 Equilibria: their feasibility and stability conditions.

Equilibrium	Feasibility conditions	Stability conditions
$E_0 = (0, 0)$	-	unstable
$E_N = (K, 0)$	-	unstable
$E_P = (0, H)$	-	unstable
$E_{NP} = (N^*, P(N^*))$	feasible:	
$P(N^*) = \Psi(N^*) = \Phi(N^*)$,	$\Psi\left(N_{\Psi'_+}\right) \geq \Phi\left(N_{\Psi'_+}\right)$	stable for
i.e.,	unfeasible:	$N^* > \max(N_\alpha^*, N_\beta^*)$
(A1) and (A2)	$\Psi\left(N_{\Psi'_+}\right) \leq H$	

4.2 | Bifurcations

We discuss here briefly the possible existence of bifurcations. The mathematical details are contained in Appendix A.2.2.

Evidently, because all the equilibria where at least one population vanishes are unstable, there cannot be any transcritical bifurcation, which instead arise for instance in [1, 3]. We now investigate the onset of persistent limit cycles. In order to have a Hopf bifurcation, we need the vanishing of the trace and a positive determinant. In view of the above discussion, we do not know the exact location of the point where the former occurs, which corresponds to $\alpha(N^*) = 0$, or $A(N^*) = B(N^*)$ in (A8). But this intersection, if it occurs, is certainly smaller than N_{A_+}, although it may be close to the vertical axis $N = 0$. On the other hand, the determinant is certainly positive for large values of N, because inequality (A9) is certainly satisfied past the value for which $C(N^*) = D(N^*)$, and the latter must be smaller than $X^0 = \max\{C^0, D^0\}$. It follows that a necessary condition for the existence of a Hopf bifurcation is

$$N_{A_+} > X^0 = \max\{C^0, D^0\}. \tag{5}$$

5 | A PREDATOR WITH TWO PREY GATHERING IN HERDS

Here, we consider two prey populations N and M, that grow logistically, with respective growth rates r and q, carrying capacities K and J, but possibly compete among each other, with generic rate c_{WQ}, $W \neq Q$, $W, Q \in \{N, M\}$ to indicate the adverse action of population Q over W. The corresponding model with no prey competition is obtained by setting to zero these rates. The predator is generalist, with reproduction rate s and carrying capacity H due to other food resources not

explicitly modeled. It hunts each prey at rate a_N, respectively, a_M, while b_N and b_M are coefficients related to the product of handling times and hunting rates. The model reads

$$\frac{dN}{dt} = rN\left(1 - \frac{N}{K}\right) - \frac{a_N\sqrt{N}P}{1 + b_N N} - c_{NM}NM, \tag{6}$$

$$\frac{dM}{dt} = qM\left(1 - \frac{M}{J}\right) - \frac{a_M\sqrt{M}P}{1 + b_M M} - c_{MN}MN, \tag{7}$$

$$\frac{dP}{dt} = sP\left(1 - \frac{P}{H}\right) + \frac{e_N a_N \sqrt{N}P}{1 + b_N N} + \frac{e_M a_M \sqrt{M}P}{1 + b_M M}. \tag{8}$$

with Jacobian matrix

$$J = \begin{bmatrix} J_{1,1} & -c_{NM}N & -\frac{a_N\sqrt{N}}{1+b_N N} \\ -c_{MN}M & J_{2,2} & -\frac{a_M\sqrt{M}}{1+b_M M} \\ J_{3,1} & J_{3,2} & s - \frac{2sP}{H} + \frac{a_N e_N\sqrt{N}}{1+b_N N} + \frac{a_M e_M\sqrt{M}}{1+b_M M} \end{bmatrix},$$

where

$$J_{1,1} = r - \frac{2rN}{K} - \frac{a_N P}{2\sqrt{N}(1 + b_N N)} + \frac{a_N b_N \sqrt{N}P}{(1 + b_N N)^2} - c_{NM}M,$$

$$J_{2,2} = q - \frac{2qM}{J} - \frac{a_M P}{2\sqrt{M}(1 + b_M M)} + \frac{a_M b_M \sqrt{M}P}{(1 + b_M M)^2} - c_{MN}N,$$

$$J_{3,1} = \frac{a_N e_N P}{2\sqrt{N}(1 + b_N N)} - \frac{a_N b_N e_N \sqrt{N}P}{(1 + b_N N)^2},$$

$$J_{3,2} = \frac{a_M e_M P}{2\sqrt{M}(1 + b_M M)} - \frac{a_M b_M e_M \sqrt{M}P}{(1 + b_M M)^2}.$$

5.1 | Equilibria

Here, a number of equilibria are easily determined. Namely, $E_0 = (0, 0, 0)$, $E_P = (0, 0, H)$, $E_M = (0, J, 0)$, $E_N = (K, 0, 0)$, that are unconditionally feasible. For the equilibrium with only predators vanishing, $E_{NM} = (N_{NM}, M_{NM}, 0)$, we find

$$E_{NM} = \left(\frac{qK(c_{NM}J - r)}{c_{NM}c_{MN}JK - qr}, \frac{rJ(c_{MN}K - q)}{c_{NM}c_{MN}JK - qr}, 0\right).$$

For feasibility, we clearly need either one of the following alternative two sets of conditions to hold:

$$c_{NM}c_{MN}JK > qr, \quad c_{NM}J \geq r, \quad c_{MN}K \geq q; \tag{9}$$

$$c_{NM}c_{MN}JK < qr, \quad c_{NM}J \leq r, \quad c_{MN}K \leq q. \tag{10}$$

which can be reduced to

$$c_{NM}J \geq r, \quad c_{MN}K \geq q; \tag{11}$$

$$c_{NM}J \leq r, \quad c_{MN}K \leq q. \tag{12}$$

The other equilibria with two nonvanishing populations,

$$E_{MP} = (0, M^*, P(M^*)), \quad E_{NP} = (N^*, 0, P(N^*)),$$

correspond to the coexistence equilibrium of the model (3)–(4), that have been already analyzed, and *mutatis mutandis* have the same feasibility conditions. More specifically,

$$P(M^*) = \Psi_M(M^*) = \Phi_M(M^*), \quad P(N^*) = \Psi_N(N^*) = \Phi_N(N^*),$$

where the functions Ψ_Q, Φ_Q, $Q \in \{M, N\}$, are the same Ψ, Φ of Section 4.1.

Also the stability conditions are inherited from the two-dimensional submodel (3)–(4), unaltered. This statement follows from the fact that, considering, for example, E_{MP}, in the three-dimensional phase space N near the equilibrium attains values close to zero; then in (6), the dominant term in the right hand side is represented by predation, modeled by the fraction, which approximately becomes $-a_N\sqrt{N}$, as $P \approx P(M^*)$, that is, a constant. Thus, the trajectories near E_{MP} must approach the $M - P$ phase plane.

The details of the coexistence equilibrium analysis are reported in Appendix A.2.1

As for stability the equilibria $E_0 = (0, 0, 0)$, $E_M = (0, J, 0)$, $E_N = (K, 0, 0)$, $E_{NM} = (N_{NM}, M_{NM}, 0)$ are all unconditionally unstable. Indeed as in the predator-prey model (3)–(4), we analyze separately the equations leading to possible singularities in the Jacobian. In any case, the above equilibria possess at least one positive eigenvalue. Denoting by λ_Q the positive eigenvalue for point E_Q, we find $\lambda_0 = s$ and

$$\lambda_M = s + \frac{a_M e_M \sqrt{J}}{1 + b_M J}, \quad \lambda_N = s + \frac{a_N e_N \sqrt{K}}{1 + b_N K},$$

$$\lambda_{NM} = s + \frac{a_N e_N \sqrt{\frac{qK(c_{NM}J - r)}{c_{NM}c_{MN}JK - qr}}}{1 + \frac{b_N qK(c_{NM}J - r)}{c_{NM}c_{MN}JK - qr}} + \frac{a_M e_M \sqrt{\frac{rJ(c_{MN}K - q)}{c_{NM}c_{MN}JK - qr}}}{1 + \frac{b_M rJ(c_{MN}K - q)}{c_{NM}c_{MN}JK - qr}}$$

while for $E_P = (0, 0, H)$ an analysis similar to the one performed for model (3)–(4) shows that the local stability depends on the relative speeds at which the three populations approach E_P, and therefore, the latter is unstable.

For both E_{NP} and E_{MP}, we must analyze separately the equation for the variable that vanishes. We find that its dominant term behaves, respectively, like qM and rN, and therefore, trajectories will drift away from the equilibrium point in the direction orthogonal to the phase plane of the two nonvanishing populations. Hence, also these equilibria are unstable. However, within the coordinate planes $M = 0$ and $N = 0$, they are stable, as demonstrated by Figure 2, for these reference parameter values

$$a_N = 0.2, \ a_M = 0.4, \ b_N = 0.8, \ b_M = 0.9, \ c_{NM} = 0.0005,$$
$$c_{MN} = 0.0007, \ e_N = 0.3, \ e_M = 0.5, \ r = 0.6, \tag{13}$$
$$q = 0.8, \ s = 0.5, \ K = 100, \ J = 150, \ H = 75.$$

The initial conditions, respectively, are for Figure 2 left:

$$N(0) = 0, \ M(0) = 30, \ P(0) = 150, \tag{14}$$

and for Figure 2 right:

$$N(0) = 50, \ M(0) = 0, \ P(0) = 150. \tag{15}$$

The details of the stability analysis of the coexistence equilibrium are reported in Appendix A.2.2. Sufficient conditions are given in (A25) and (A26).

The fact that both feasibility and stability conditions of this coexistence equilibrium can be simultaneously satisfied is shown through numerical simulations, shown in Figure 3, again for the parameter values (13) and for the initial conditions

$$N(0) = 30, \ M(0) = 30, \ P(0) = 30. \tag{16}$$

For different predators carrying capacities, H, the latter can attain values larger than both prey, an intermediate value or smaller than both. A symmetric picture with the role of the two prey (red and green trajectories) can also be obtained, not shown.
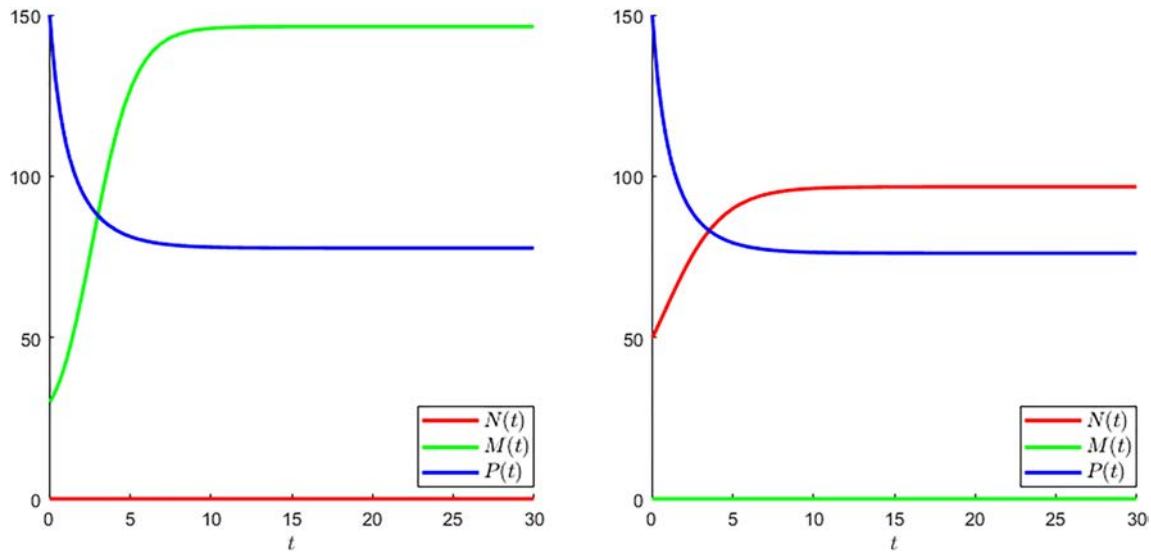
FIGURE 2 Here, the two equilibria E_{MP} (left) and E_{NP} (right) are shown to be stable in the respective coordinate planes, if the initial conditions are chosen in these planes, namely, (14) and (15). The figures are constructed with the parameter values (13). Note that these equilibria in the phase space are anyway unstable. [Colour figure can be viewed at wileyonlinelibrary.com]
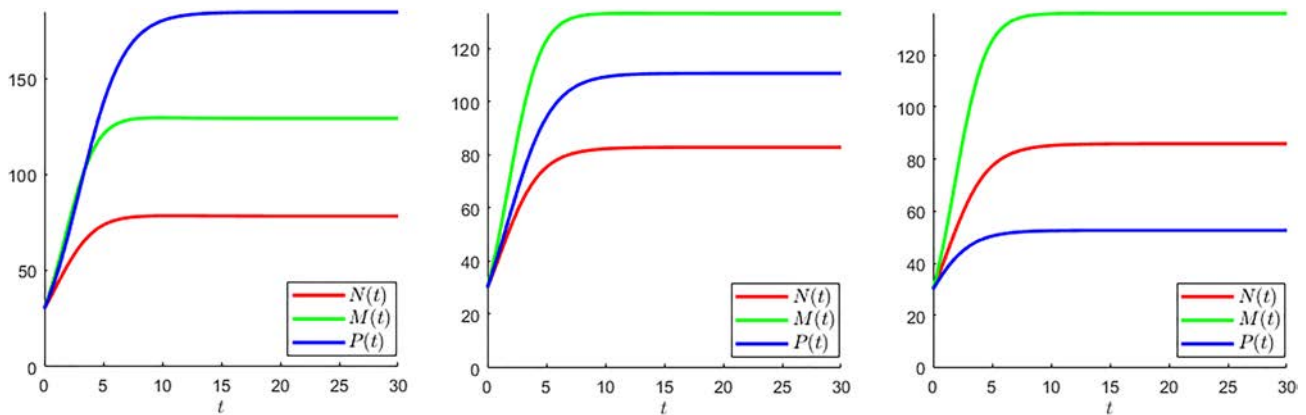
FIGURE 3 Coexistence for model obtained for the parameter values (13), with the exception of H which attains the values $H = 175$ (left), $H = 105$ (center), $H = 50$ (right), and the initial conditions (16). [Colour figure can be viewed at wileyonlinelibrary.com]

6 | A PREDATOR, AN INDIVIDUALISTIC PREY, AND A PREY GATHERING IN HERDS

In this case, we consider again an individualistic-behaving predator together with two prey. Keeping the same notation as in Section 5, the difference with model (6)–(8) is the fact that here N still gathers in a herd, while M does not. Hence, the predators' interactions with the latter occur on a one-to-one basis as in the classical Lotka-Volterra model. We assume logistic trend for each of the three populations in the absence of the other two, and interspecific competition for environmental resources between the two prey populations, as we did in Section 5. Thus, the model reads

$$\frac{dN}{dt} = rN\left(1 - \frac{N}{K}\right) - \frac{a_N\sqrt{N}P}{1 + b_N N} - c_{NM}NM \tag{17}$$

$$\frac{dM}{dt} = qM\left(1 - \frac{M}{J}\right) - \frac{a_M MP}{1 + b_M M} - c_{MN}MN \tag{18}$$

$$\frac{dP}{dt} = sP\left(1 - \frac{P}{H}\right) + \frac{e_N a_N\sqrt{N}P}{1 + b_N N} + \frac{e_M a_M MP}{1 + b_M M}. \tag{19}$$

6.1 | Equilibria

The analysis follows pretty much the same approach of Section 5. We therefore just highlight the basic results, without providing all the details. All the equilibria in which one population vanishes are unstable.

Again, we can show that the boundary equilibria can be achieved for the parameter values (29) if the initial conditions are chosen in their respective coordinate planes, namely, for

$$N(0) = 0, \ M(0) = 250, \ P(0) = 450, \tag{20}$$

for the herding-prey-free equilibrium while for the individualistic-prey-free equilibrium, they are the same used in the previous section, namely, (15). In this case, however, we do not show the pictures.

We therefore concentrate only on the study of coexistence. From the first equilibrium equation, we obtain the function Λ of (A15); from the second one, we obtain

$$P = \frac{1}{a_M} \left(q \left(1 - \frac{M}{J} \right) - c_{MN} N \right) (1 + b_M M) = \Xi(N, M), \tag{21}$$

and from the last one,

$$\Upsilon_{NM}(N, M) = H + \frac{a_N e_N H \sqrt{N}}{s(1 + b_N N)} + \frac{a_M e_M H M}{s(1 + b_M M)}. \tag{22}$$

Coexistence is obtained by the intersection of these surfaces, $E_{NMP} = (N^*, M^*, P(N^*, M^*))$, where

$$P(N^*, M^*) = \Lambda(N^*, M^*) = \Xi(N^*, M^*) = \Upsilon_{NM}(N^*, M^*). \tag{23}$$

Evaluating the gradient of $\Upsilon_{NM}(N, M)$, it is seen that its second component never vanishes, so that no extremal points exist in the first quadrant. Its minimum occurs on the boundary of the domain, with value H, at the origin $(0, 0)$, and maximum value

$$\Upsilon_{NM_{\max}} = H + \frac{a_N e_N H}{2s\sqrt{b_N}} + \frac{a_M e_M H J}{s(1 + b_M J)}, \tag{24}$$

assuming the first term attaining its maximal value for $N = b_N^{-1}$, while the second one is a function always increasing in M.

To investigate Ξ again, we find that the first component of its gradient is always negative, so that no possible extrema exist, except for the boundary of the domain. Now, on the coordinate plane $N = 0$, this surface becomes the concave parabola

$$\Gamma(M) = -\frac{q}{a_M J} \left(b_M M^2 + (1 - b_M J) M - J \right). $$

through the point $\left(0, q a_M^{-1} \right)$ and thus with one positive root, $M_{\Gamma_+} = J$. The vertex is located at the abscissa

$$M_{\Gamma_V} = -\frac{1 - b_M J}{2 b_M} = \frac{1}{2} \left(J - \frac{1}{b_M} \right), \tag{25}$$

positive if and only if $J > \frac{1}{b_M}$ and height

$$\Gamma(M_{\Gamma_V}) = \frac{q}{2 a_M J} \left(\frac{1}{2} b_M J^2 + \frac{1}{2 b_M} + J \right). \tag{26}$$

The maximum of the parabola is the height $\Gamma(M_{\Gamma_V})$ of the vertex $\left(M_{\Gamma_V}, \Gamma(M_{\Gamma_V}) \right)$ if $b_M J > 1$ and the height at the origin $\left(0, q a_M^{-1} \right)$, conversely.

Thus, $\Gamma(M)$ has only two possible behaviors, increasing up to the maximum or steadily decreasing.

From the above considerations, it is thus found that the minimum of Ξ is 0 while the maximum is

$$\Xi\left(0, \max\{0, M_{\Gamma_V}\} \right) = \max\left\{ \Xi(0, 0), \Xi(0, M_{\Gamma_V}) \right\} = \max\left\{ \frac{q}{a_M}, \Gamma(M_{\Gamma_V}) \right\}, \tag{27}$$
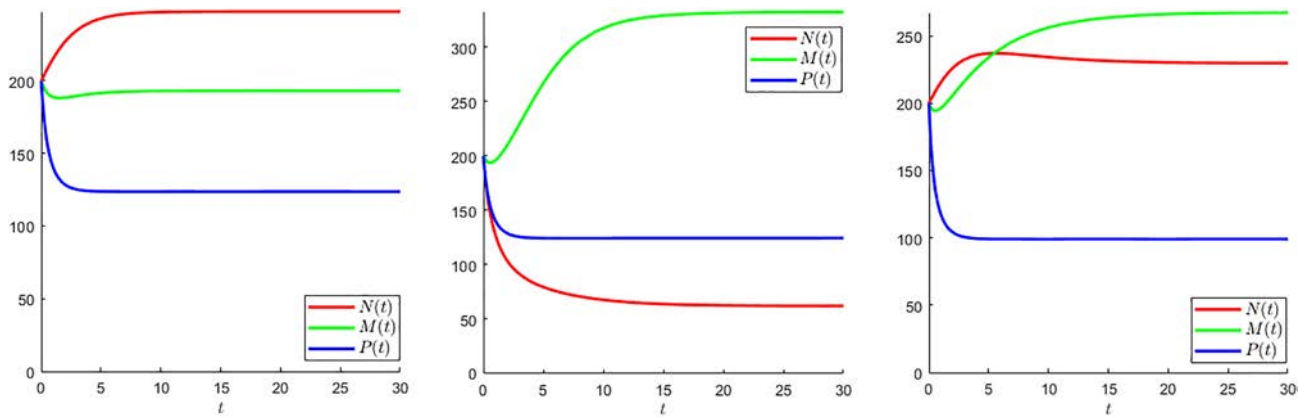
FIGURE 4 Coexistence is obtained by the parameter values (29) and the initial conditions (30), with the remaining carrying capacities for the prey N and the predators given by $K = 300$ and $H = 100$ (left), $K = 100$ and $H = 100$ (center), $K = 300$ and $H = 80$ (right). [Colour figure can be viewed at wileyonlinelibrary.com]

Since $\Upsilon_{NM}(N, M)$ has the minimum H in the first quadrant, a sufficient condition for the nonexistence of E_{NMP} is $h_{\min} < H$, with

$$h_{\min} = \min\left\{ \Psi_N\left(N_{\Psi'_{N_+}}\right), \Xi\left(0, \max\{0, M_{\Gamma_V}\}\right) \right\}. \tag{28}$$

In Figure 4, we show that the coexistence equilibrium can indeed be stably achieved, for the parameter values

$$a_N = 0.2, \ a_M = 0.4, \ b_N = 0.8, \ b_M = 0.9, \ e_N = 0.3,$$
$$e_M = 0.5, \ c_{NM} = 0.0005, \ c_{MN} = 0.0007, \ r = 0.6, \ q = 0.8, \tag{29}$$
$$s = 0.95, \ J = 450$$

and initial conditions

$$N(0) = 200, \ M(0) = 200, \ P(0) = 200. \tag{30}$$

7 | DISCUSSION

We discuss here the results obtained in terms of corresponding studies that have already appeared in the literature. We especially focus on the coexistence equilibrium of the two-population system, so as to better illustrate the differences pictorially.

In all the models considered in the literature, focusing in particular on those examined in [1–3] and [4], the predators are assumed to be specialist. Therefore, a direct comparison is not completely possible. Indeed, in all the above cited papers, the prey-free equilibrium does not exist, while it is allowed in (3)–(4), because here the predators are generalist and thrive on the other resources even in the absence of the prey modeled in the system. On the other hand, in our model, this last prey-free point is unconditionally unstable, so that this difference in the formulation is not too much relevant in practical terms. More important, in [1] as well as in [3], a transcritical bifurcation is shown between the predator-free point and the coexistence equilibrium. In the system proposed here, (3)–(4), this is impossible, because the predator-free equilibrium is always unstable. The transcritical bifurcation of [1] occurs for the critical value of the specialist predators mortality

$$m^\dagger = ae\sqrt{K}$$

while the one in [3] is

$$m^\ddagger = \frac{ae\sqrt{K}}{1 + b\sqrt{K}}$$

The only equilibrium that is common to all models, [1] and [3] as well as (3)–(4), and behaves in the same way is the origin, which turns out to be always unconditionally unstable.
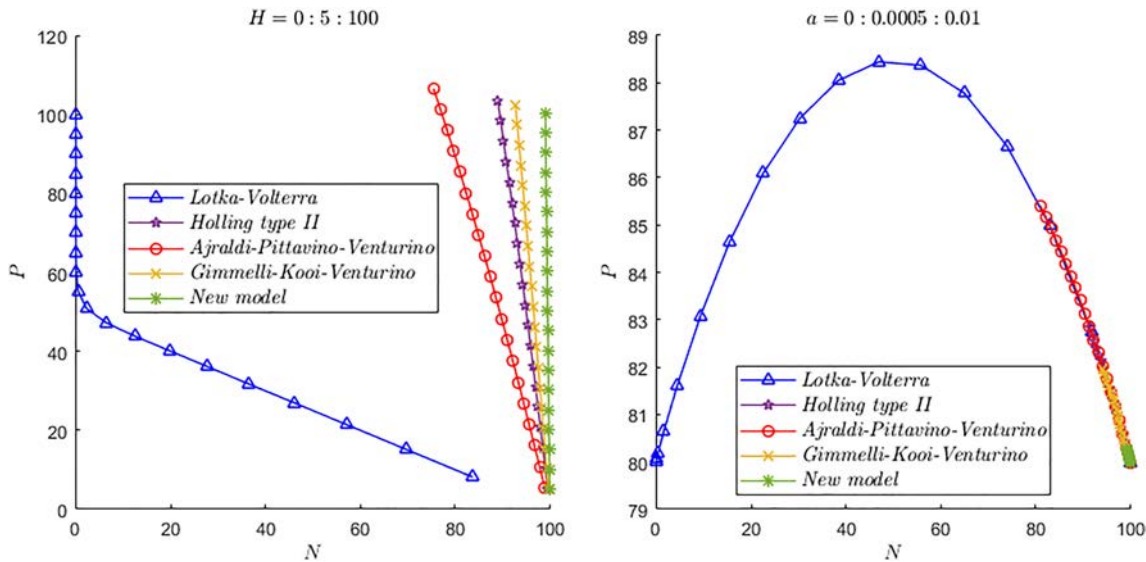
FIGURE 5 Left: We vary the predators carrying capacity $H \in [0, 100]$. Right: We vary the predators hunting rate $a \in [0, 0.01]$. The other parameters are given by (33) and initial conditions (34). [Colour figure can be viewed at wileyonlinelibrary.com]
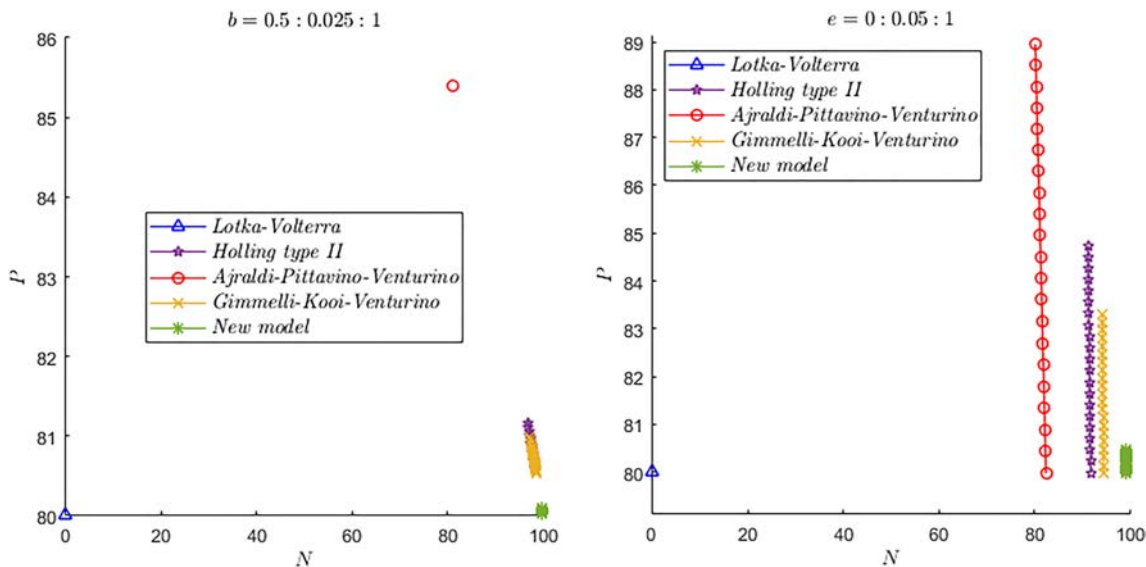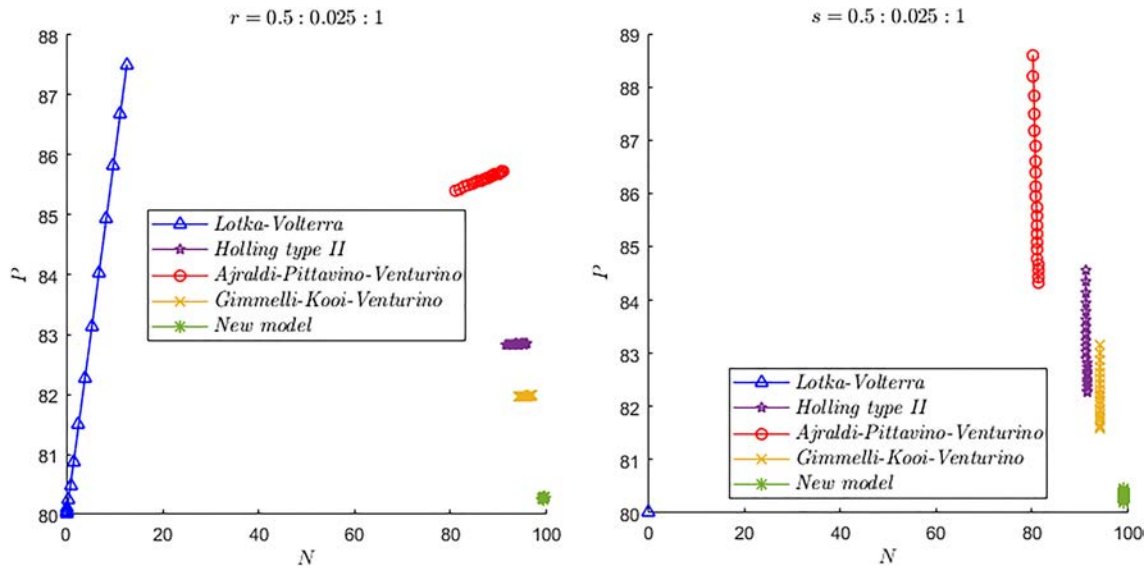

FIGURE 6 Left: We vary the parameter $b \in [0.5, 1.0]$. Right: We vary the conversion coefficient $e \in [0, 1.0]$. The other parameters are given by (33) and initial conditions (34). [Colour figure can be viewed at wileyonlinelibrary.com]

In any case, we reformulate here both models of [1] and [3] so as to use generalist predators, to make the comparison of the three situations fair. Thus, the model in [1] is reformulated as follows

$$
\begin{aligned}
\frac{dN}{dt} &= rN\left(1 - \frac{N}{K}\right) - a\sqrt{N}P \\
\frac{dP}{dt} &= sP\left(1 - \frac{P}{H}\right) + ae\sqrt{N}P,
\end{aligned}
\tag{31}
$$

while the one in [3] becomes

$$
\begin{aligned}
\frac{dN}{dt} &= rN\left(1 - \frac{N}{K}\right) - \frac{a\sqrt{N}P}{1 + b\sqrt{N}} \\
\frac{dP}{dt} &= sP\left(1 - \frac{P}{H}\right) + \frac{ae\sqrt{N}P}{1 + b\sqrt{N}}.
\end{aligned}
\tag{32}
$$

FIGURE 7 Left: We vary the prey reproduction rate $r \in [0.5, 1.0]$. Right: We vary the predators reproduction rate $s \in [0.5, 1.0]$. The other parameters are given by (33) and initial conditions (34). [Colour figure can be viewed at wileyonlinelibrary.com]

An analytic comparison of the coexistence population levels is not possible either, because the latter are available in [1] and [3], but not in the model presented here. This issue must then be investigated numerically. More specifically, replace in both (31) and (32) the logistic parts for the predators with their natural mortality m. Before proceeding in with the simulations of coexistence, we recall the coexistence equilibria (N^*, P^*) and (N^{**}, P^{**}), respectively, [1] and [3]. For [1], we then find coexistence at the population levels

$$N^* = \frac{m^2}{a^2 e^2}, \ P^* = \frac{r}{a} \sqrt{N^*} \left(1 - \frac{N^*}{K} \right),$$

while for [3], we have

$$N^{**} = \frac{m^2}{(ae - bm)^2}, \ P^{**} = \frac{r}{a} \sqrt{N^{**}} \left(1 - \frac{N^{**}}{K} \right) \left(1 + b\sqrt{N^{**}} \right).$$

In what follows, we show the behavior of the quadratic Lotka-Volterra model for generalist predators, that is, incorporating a logistic term due to the alternative food resources, the corresponding HTII model, model (31), model (32), and (3)–(4). We take the following parameter values as reference

$$a = 0.01, \ b = 0.2, \ e = 0.6, \ r = 0.5, \ s = 0.8, \ H = 80, \ K = 100 \tag{33}$$

and initial conditions for all Figures 5, 6, and 7:

$$N(0) = 50, \ P(0) = 10. \tag{34}$$

We vary one of the parameters at the time, always keeping the prey carrying capacity fixed. The results are shown in Figures 5, 6, and 7.

The insight we gather from these experiments is that the model proposed here always shows that the prey thrive in larger numbers, as the plots of the steady states in this case lie always on the right of all the other ones. This outcome ecologically should be expected, but it is important that also the mathematics validates the intuitive thoughts.

ACKNOWLEDGEMENTS

CONFLICT OF INTEREST STATEMENT

This work does not have any conflicts of interest.

ORCID

Francesca Acotto https://orcid.org/0000-0003-3807-5916
Ezio Venturino https://orcid.org/0000-0001-7215-5114

REFERENCES

1. V. Ajraldi, M. Pittavino, and E. Venturino, *Modeling herd behavior in population systems*, Nonlinear Anal. Real. World Appl. **12** (2011), 2319–2338.
2. P. A. Braza, *Predator prey dynamics with square root functional responses*, Nonlinear Anal. Real World Appl. **13** (2012), 1837–1843.
3. G. Gimmelli, B. W. Kooi, and E. Venturino, *Ecoepidemic models with prey group defense and feeding saturation*, Ecological Complexity **22** (2015), 50–58.
4. S. P. Bera, A. Maiti, and G. Samanta, *Modelling herd behavior of prey: analysis of a prey-predator model*, World J. Model. Simul. **11** (2015), no. 1, 3–14.
5. V. Capasso and G. Serio, *A generalization of the Kermack-Mckendrick deterministic epidemic model*, Math. Biosci. **42** (1978), 43–61.
6. T. Caro, *Antipredator defenses in birds and mammals*, University of Chicago Press, Chicago, 2005.
7. T. Pitcher and G. Turner, *Attack abatement: a model for group protection by combined avoidance and dilution*, Am. Nat. **128** (1986), 228–240.
8. S. Lima, *Back to the basics of anti-predatory vigilance: the group-size effect*, Anim. Behav. **49** (1995), 11–20.
9. G. Roberts, *Why individual vigilance increases as group size increases*, Anim. Behav. **51** (1996), 1077–1086.
10. R. Heller and H. Milinski, *Influence of a predator on the optimal foraging behavior of sticklebacks*, Nature **275** (1978), 642–644.
11. H. S. Clements, G. I. Kerley, and C. J. Tambling, *Prey morphology and predator sociality drive predator prey preferences*, J. Mammal. **97** (2016), 919–927.
12. I. M. Bulai and E. Venturino, *Shape effects on herd behavior in ecological interacting population models*, Math. Comput. Simul. **141** (2017), 40–55, DOI 10.1016/j.matcom.2017.04.009.
13. C. S. Holling, *The functional response of invertebrate predators to prey density*, Mem Entomol Soc Can. **45** (1965), 3–60.
14. L. Michaelis and M. L. Menten, *Die Kinetik der Invertinwirkung*, Biochem. Z. **49** (1913), 333–369.
15. S. Belvisi and E. Venturino, *An ecoepidemic model with diseased predators and prey group defense*, Simul. Model Pract. Theory **34** (2013), 144–155.
16. S. Saha and G. P. Samanta, *Analysis of a predator-prey model with herd behavior and disease in prey incorporating prey refuge*, Int. J. Biomath. **12** (2019), no. 1, 1950007, DOI 10.1142/S1793524519500074.
17. D. Melchionda, E. Pastacaldi, C. Perri, and E. Venturino, *Social behavior-induced multistability in minimal competitive ecosystems*, J. Theor. Biol. **439** (2018), 24–38.
18. T. Singh and S. Banerjee, *Spatiotemporal model of a predator-prey system with herd behavior and quadratic mortality*, Int. J. Bifurcation Chaos **29** (2019), no. 04, 1950049, DOI 10.1142/S0218127419500494.
19. Fethi Souna and Abdelkader Lakmeche, *Spatiotemporal patterns in a diffusive predator-prey system with Leslie-Gower term and social behavior for the prey*, Math. Meth. Appl Sci. **44** (2021), 13920–13944.
20. F. Souna, S. Djilali, and F. Charif, *Mathematical analysis of a diffusive predator-prey model with herd behavior and prey escaping*, Math. Model Nat. Phenom. **15** (2020), 23, DOI 10.1051/mmnp/2019044.
21. F. Souna, S. Djilali, and A. Lakmeche, *Spatiotemporal behavior in a predator-prey model with herd behavior and cross-diffusion and fear effect*, Eur. Phys. J. Plus **136** (2021). Article number: 474.
22. S. Yuan, C. Xu, and T. Zhang, *Spatial dynamics in a predator-prey model with herd behavior*, Chaos **23** (2013), no. 033201, DOI 10.1063/1.4812724.
23. M. Reed and B. Simon, *Methods of modern mathematical physics*, Vol. **4**, Academic Press, Analysis of Operators, New York, 1978.
24. G. Schaller, *The Serengeti lion: a study of predator-prey relations*, University of Chicago Press, Chicago, 1972.

APPENDIX A: PREDATOR AND A HERD OF PREY

A.1 | Coexistence feasibility

To find coexistence $E_{NP} = (N^*, P(N^*))$, we need to intersect the following curves, arising from the equilibrium equations:

$$\Psi(N) = \frac{r}{a} \sqrt{N} \left(1 - \frac{N}{K} \right) (1 + bN) \tag{A1}$$

$$\Phi(N) = H + \frac{aeH\sqrt{N}}{s(1 + bN)} \tag{A2}$$

so that, ultimately $P(N^*) = \Psi(N^*) = \Phi(N^*)$.

Now, $\Psi(N)$ has the zeros $N_{\Psi_1} = 0$ and $N_{\Psi_2} = K$. Its derivative

$$\frac{d\Psi(N)}{dN} = -\frac{r[5bN^2 - 3(bK - 1)N - K]}{2aK\sqrt{N}}.$$

It is nonnegative if the numerator is. The latter is a quadratic, with roots

$$N_{\Psi'_\pm} = \frac{3(bK - 1) \pm \sqrt{\Delta_{\Psi'}}}{10b},$$

where the discriminant is always positive, $\Delta_{\Psi'} = 9(bK - 1)^2 + 20bK > 0$. Thus, $\Psi(N)$ is increasing for $N_{\Psi'_-} < 0 < N < N_{\Psi'_+}$, decreasing instead for $N > N_{\Psi'_+}$, with $\lim_{N \to +\infty} \Psi(N) = -\infty$. The function has thus a unique maximum at $\tilde{N} = N_{\Psi'_+}$ and is nonnegative in $[0, K]$. From its second derivative

$$\frac{d^2\Psi(N)}{dN^2} = -\frac{r[15bN^2 - 3(bK - 1)N + K]}{4aKN\sqrt{N}},$$

with roots

$$N_{\Psi''_\pm} = \frac{3(bK - 1) \pm \sqrt{\Delta_{\Psi''}}}{30b},$$

where

$$\Delta_{\Psi''} = 9(bK - 1)^2 - 60bK = 3(3b^2K^2 - 26bK + 3).$$

Now, $\Delta_{\Psi''} \geq 0$ whenever one of the following conditions are satisfied: $0 < 3bK \leq 13 - 4\sqrt{10}$ or $3bK \geq 13 + 4\sqrt{10}$, and furthermore $\Delta_{\Psi''} \geq (3bK - 3)^2$ if and only if $bK \leq 0$.

In summary, for $3bK \geq 13 + 4\sqrt{10}$, Ψ has two inflection points, being concave for $0 < N < N_{\Psi''_-}$ or $N > N_{\Psi''_+}$ and convex in the interval $[N_{\Psi''_-}, N_{\Psi''_+}]$. For $3bK < 13 + 4\sqrt{10}$ instead, it is always convex.

The function $\Phi(N)$, its domain being $N \geq 0$, starts from the point $(0, H)$ and tends to the horizontal asymptote $P = H$ and never vanishes. Differentiating, we find that it is increasing in $[0, b^{-1}]$, with a maximum at the right endpoint, with height

$$\Phi\left(\frac{1}{b}\right) = H + \frac{aeH}{2\sqrt{bs}}.$$

From its second derivative, we find the inflection points

$$N_{\Phi''_-} = \frac{1}{b}\left(1 - \frac{2\sqrt{3}}{3}\right) < 0, \quad N_{\Phi''_+} = \frac{1}{b}\left(1 + \frac{2\sqrt{3}}{3}\right) > 0,$$

so that it is concave in $\left[0, N_{\Phi''_+}\right]$ and convex for $N > N_{\Phi''_+}$. Figure A1 shows the behaviors of both functions $\Psi(N)$ and $\Phi(N)$.

We now study the possible intersections among Ψ and Φ in the first quadrant, which can be at most four. Clearly, no intersection is possible if $\Psi\left(N_{\Psi'_+}\right) \leq H$. A sufficient condition for at least one intersection is instead $\Psi\left(N_{\Psi'_+}\right) \geq \Phi\left(N_{\Psi'_+}\right)$.
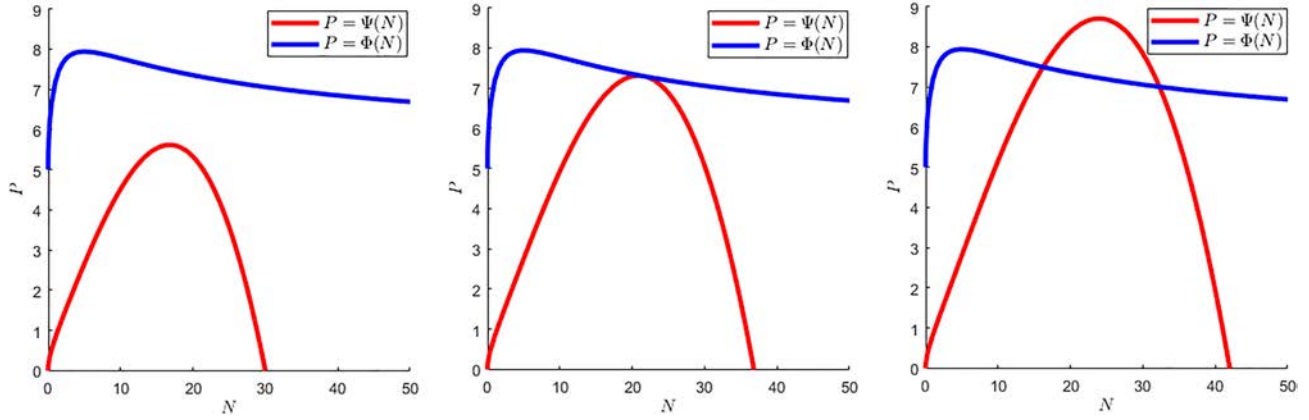
FIGURE A1 Illustration of the saddle-node bifurcation: graphs of the functions $\Phi(N)$ e $\Psi(N)$, with the parameter values $a = 0.7$, $b = 0.2$, $e = 0.3$, $r = 0.5$, $s = 0.4$, and $H = 5$, where, left to right, the prey carrying capacity attains the values $K = 30$, $K = 36.8$, and $K = 42$. [Colour figure can be viewed at wileyonlinelibrary.com]

Evaluating the functions at the point $N_{\Psi'_+}$, the above sufficient condition for the intersection to occur explicitly becomes

$$\sqrt{\frac{3(bK - 1) + \sqrt{\Delta_{\Psi'}}}{10b}} \geq \frac{100absHK\left(7 + 3bK + \sqrt{\Delta_{\Psi'}}\right)}{D}, \tag{A3}$$

where

$$D = rs\left(7bK + 3 - \sqrt{\Delta_{\Psi'}}\right)\left(7 + 3bK + \sqrt{\Delta_{\Psi'}}\right)^2 - 1000a^2beHK \in \mathbf{R},$$

while the one guaranteeing instead that coexistence is not possible is

$$\sqrt{\frac{3(bK - 1) + \sqrt{\Delta_{\Psi'}}}{10b}} \leq \frac{100abHK}{r\left(7bK + 3 - \sqrt{\Delta_{\Psi'}}\right)\left(7 + 3bK + \sqrt{\Delta_{\Psi'}}\right)}. \tag{A4}$$

In the transition between the two configurations, for $\Psi\left(N_{\Psi'_+}\right) = \Phi\left(N_{\Psi'_+}\right)$ a saddle-node bifurcation occurs, see Figure A1 where it is shown taking K as bifurcation parameter.

A.2 | Coexistence stability

Using the equilibrium equations, the diagonal terms of J evaluated at the equilibrium E_{NP} simplify somewhat,

$$J_{NP_{1,1}} = \frac{r}{2} - \frac{3rN^*}{2K} + \frac{brN^*}{1 + bN^*}\left(1 - \frac{N^*}{K}\right),$$

$$J_{NP_{2,2}} = -s - \frac{ae\sqrt{N^*}}{1 + bN^*}.$$

providing the trace and the determinant

$$\mathrm{tr}\,(J_{NP}) = \frac{\alpha(N^*)}{2K(1 + bN^*)}, \quad \det(J_{NP}) = \frac{\beta(N^*)}{2K(1 + bN^*)^2},$$

with

$$\alpha(N^*) = K(r - 2s) - 5br(N^*)^2 + (bK(3r - 2s) - 3r)N^* - 2aeK\sqrt{N^*}, \tag{A5}$$

$$\beta(N^*) = 5b^2rs(N^*)^3 + brs(8 - 3bK)(N^*)^2 + rs(3 - 4bK)N^* \\ + 6aber(N^*)^2\sqrt{N^*} + 2aer(1 - 2bK)N^*\sqrt{N^*} - rsK. \tag{A6}$$

The Routh-Hurwitz conditions guarantee stability for

$$\operatorname{tr}(J_{NP}) < 0, \quad \det(J_{NP}) > 0,$$

which, respectively, become

$$\alpha(N^*) < 0, \quad \beta(N^*) > 0. \tag{A7}$$

The first above inequality can be restated as

$$A(N^*) < B(N^*) = 2aeK\sqrt{N^*}, \tag{A8}$$

where

$$A(N^*) = -5br(N^*)^2 + (bK(3r - 2s) - 3r)N^* + K(r - 2s).$$

The function A is a concave parabola through the point $(0, K(r - 2s))$, which has a positive height for $r > 2s$, vertex

$$V_A = \left(\frac{bK(3r - 2s) - 3r}{10br}, \frac{\Delta_A}{20br} \right),$$

with

$$\Delta_A = (bK(3r - 2s) - 3r)^2 + 20brk(r - 2s)b^2K^2(3r - 2s)^2 + 9r^2 + 2brK(r - 14s),$$

and roots

$$N_{A_\pm}^* = \frac{bK(3r - 2s) - 3r \pm \sqrt{\Delta_A}}{10br}.$$

The function $B(N^*)$ is instead a square root, a concave function, with a cusp at the origin and growing up to infinity.

For the relative positions of these functions, there are four possible situations, shown in Figure A2, but in all of them, a value $N_\alpha^* > 0$ exists for which (A8) holds.

We rewrite the second inequality in (A7) as

$$C(N^*) > D(N^*), \tag{A9}$$

where

$$C(N^*) = 5b^2rs(N^*)^3 + brs(8 - 3bK)(N^*)^2 + rs(3 - 4bK)N^* - rsK,$$
$$D(N^*) = -2aerN^*\sqrt{N^*}(3bN^* + 1 - 2bK).$$

Now the function C is a cubic that grows to $+\infty$ from $C(0) = -rsK$, thereby ensuring a positive root C^0 beyond which a feasible branch exists. This is unique, as the zeros of its derivative are

$$N_{C'_\pm}^* = \frac{3bK - 8 \pm \sqrt{\delta_{C'}}}{15b}, \quad \delta_{C'} = 9b^2K^2 + 12bK + 15K + 19$$

and further, the root $N_{C'_-}^*$ giving the position of the local maximum is negative, in view of the fact that the inequality $\sqrt{\delta_{C'}} > 3bK - 8$ is always satisfied.

The function D is positive only in the interval $[0, D^0] = [0, (2bK - 1)(3b)^{-1}]$, which is nonempty if $2bK > 1$. Thus, there always exists a point $N_\beta^* > 0$ for which $\beta(N^*) > 0$ if and only if $N^* > N_\beta^*$. The point N_β^* coincides with the zero of C if $D(x) < 0$ for $x > 0$, else it is the maximum between the intersection of C and D and the zero C^0 of C.

Summing up, (A7) holds, implying the stability of E_{NP}, if

$$N^* > \max\{N_\alpha^*, N_\beta^*\}. \tag{A10}$$
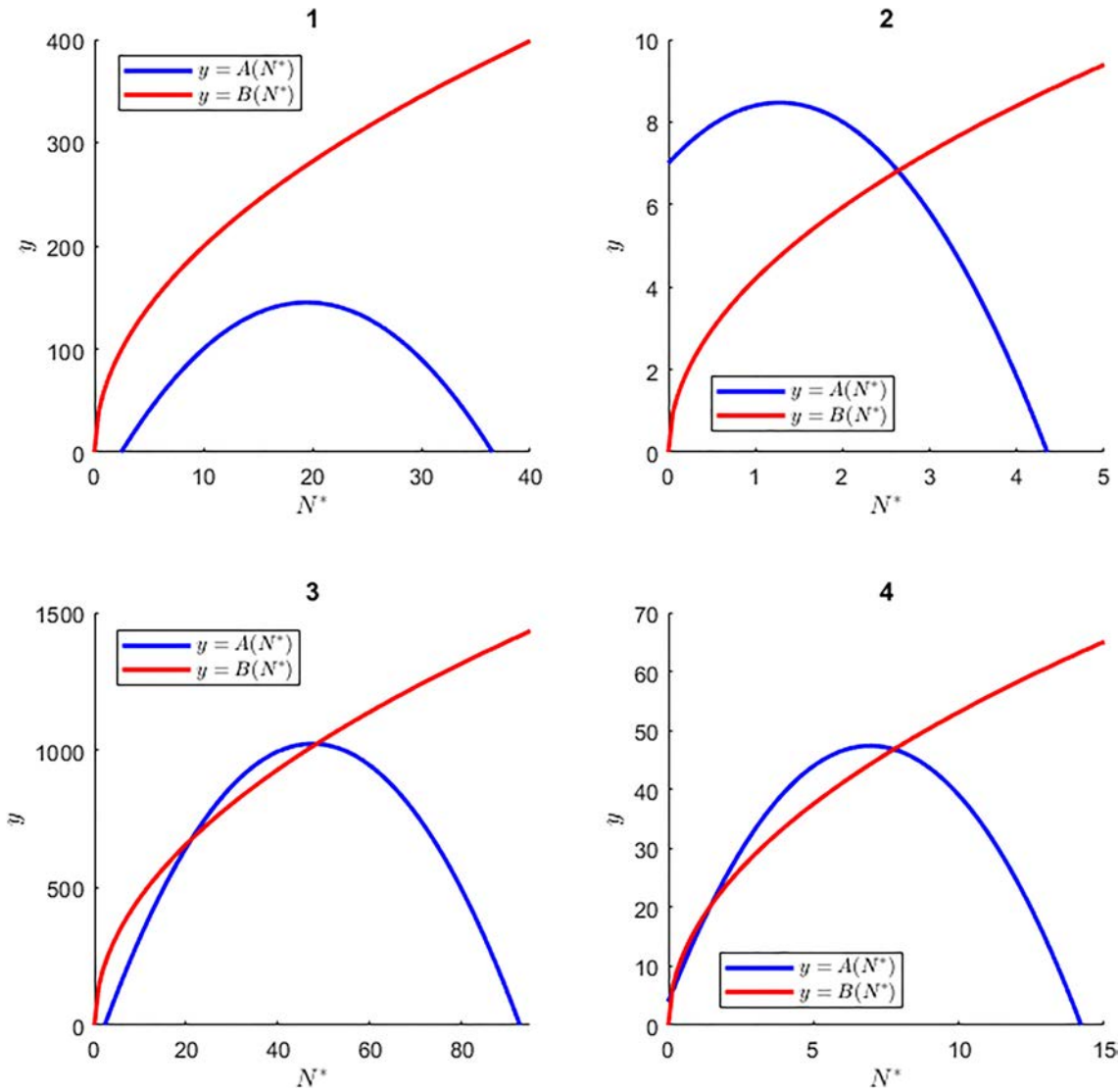
FIGURE A2 The functions $A(N^*)$ and $B(N^*)$, for $a = 0.7$, $b = 0.2$, $e = 0.3$ and: $r = 0.5$, $s = 0.4$, $K = 150$ in frame 1, $r = 0.9$, $s = 0.1$, $K = 10$ in frame 2, $r = 0.5$, $s = 0.4$, $K = 350$ in frame 3, $r = 0.9$, $s = 0.4$, $K = 40$ in frame 4. Thus, in frame 1, the inequality (A8) holds for every $N^* > 0$; in frame 2, there exists $N_1^* > 0$ such that (A8) holds for $N^* > N_1^*$; in frame 3, there exist $N_2^* > N_1^* > 0$ for which (A8) holds either for $0 < N^* < N_1^*$ or $N^* > N_2^*$; in frame 4, there exist $N_3^* > N_2^* > N_1^* > 0$ for which (A8) holds either for $N_1^* < N^* < N_2^*$ or $N^* > N_3^*$. [Colour figure can be viewed at wileyonlinelibrary.com]
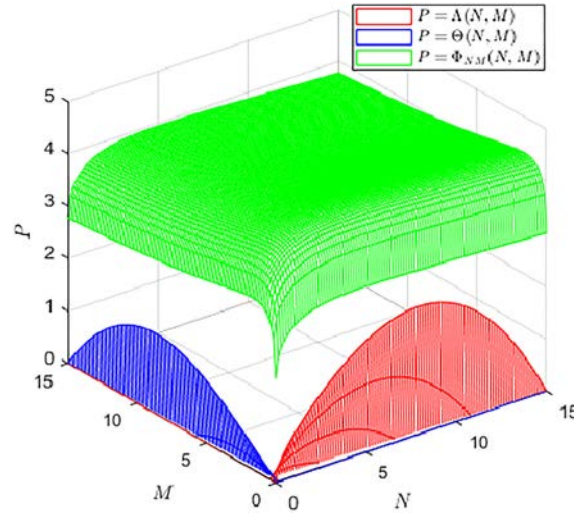
APPENDIX B: TWO HERDS OF PREY

B.1 │ Coexistence feasibility

For coexistence, from (6) and (7), we find

$$P = \frac{1}{a_N}\sqrt{N}\left(r\left(1 - \frac{N}{K}\right) - c_{NM}M\right)(1 + b_N N) = \Lambda(N, M) \tag{A11}$$

and

$$P = \frac{1}{a_M}\sqrt{M}\left(q\left(1 - \frac{M}{J}\right) - c_{MN}N\right)(1 + b_M M) = \Theta(N, M). \tag{A12}$$

FIGURE B1 The surfaces $\Lambda(N, M)$, $\Theta(N, M)$ e $\Phi_{NM}(N, M)$, for $a_N = 0.7$, $a_M = 0.5$, $b_N = 0.2$, $b_M = 0.6$, $c_{NM} = 0.9$, $c_{MN} = 0.4$, $e_N = 0.3$, $e_M = 0.8$, $q = 0.1$, $r = 0.5$, $s = 0.4$, $H = 2$, $J = 15$ and $K = 15$. [Colour figure can be viewed at wileyonlinelibrary.com]

and furthermore

$$P = H + \frac{a_N e_N H \sqrt{N}}{s(1 + b_N N)} + \frac{a_M e_M H \sqrt{M}}{s(1 + b_M M)} = \Phi_{NM}(N, M). \tag{A13}$$

The coexistence equilibrium $E_{NMP} = (N^*, M^*, P(N^*, M^*))$, if it exists, will be the intersection of these three surfaces, with

$$P(N^*, M^*) = \Lambda(N^*, M^*) = \Theta(N^*, M^*) = \Phi_{NM}(N^*, M^*). \tag{A14}$$

For the first one, we have

$$\Lambda(N, M) = \frac{\sqrt{N}}{a_N} \left(r + r \left(b_N - \frac{1}{K} \right) N - \frac{b_N r}{K} N^2 - c_{NM}(1 + b_N N)M \right), \tag{A15}$$

with the components of the gradient given by

$$\frac{\partial \Lambda(N, M)}{\partial N} = \frac{rK + 3r(b_N K - 1)N - 5b_N rN^2 - c_{NM}K(1 + 3b_N N)M}{2a_N K \sqrt{N}}$$

$$\frac{\partial \Lambda(N, M)}{\partial M} = -\frac{c_{NM}}{a_N} \sqrt{N}(1 + b_N N).$$

For $N \geq 0$, the latter never vanishes, so that no extremal points exist in the first quadrant, but for the boundary of the domain. Observe that $\Lambda(0, M) = 0$ as well as $\Lambda(N, 0) = \Psi_N(N)$, with this latter function having a maximum at $N_{\Psi'_{N_+}}$. Thus, the surface $\Lambda(N, M)$, see Figure B1, in the first quadrant has 0 as minimum value and the maximum

$$\Psi_N \left(N_{\Psi'_{N_+}} \right) = \frac{r}{a_N} \sqrt{N_{\Psi'_{N_+}}} \left(1 - \frac{N_{\Psi'_{N_+}}}{K} \right) \left(1 + b_N N_{\Psi'_{N_+}} \right). \tag{A16}$$

For the second surface $P = \Theta(N, M)$, we have

$$\Theta(N, M) = \frac{\sqrt{M}}{a_M} \left(q + q \left(b_M - \frac{1}{J} \right) M - \frac{b_M q}{J} M^2 - c_{MN}(1 + b_M M)N \right) \tag{A17}$$

with gradient components

$$\frac{\partial \Theta(N, M)}{\partial N} = -\frac{c_{MN}}{a_M} \sqrt{M}(1 + b_M M),$$

$$\frac{\partial \Theta(N, M)}{\partial M} = \frac{qJ + 3q(b_M J - 1)M - 5b_M qM^2 - c_{MN}J(1 + 3b_M M)N}{2a_M J \sqrt{M}}.$$

The first component never vanishes in the first quadrant, so that no extremal values exist, except on the boundary, for which $\Theta(N, 0) = 0$ and $\Theta(0, M) = \Psi_M(M)$, the latter with a maximum for $M_{\Psi'_{M_+}}$. Hence, $\Theta(N, M)$, see Figure B1, has 0 as minimum and attains the maximum value

$$\Psi_M \left(M_{\Psi'_{M_+}} \right) = \frac{q}{a_M} \sqrt{M_{\Psi'_{M_+}}} \left(1 - \frac{M_{\Psi'_{M_+}}}{J} \right) \left(1 + b_M M_{\Psi'_{M_+}} \right) \tag{A18}$$

Combining this information with the fact that H is the minimum value of $\Phi_{NM}(N, M)$ in the first quadrant, a sufficient condition for the nonexistence of the equilibrium E_{NMP} is $h_{\min} < H$, with

$$h_{\min} = \min \left\{ \Psi_N \left(N_{\Psi'_{N_+}} \right), \Psi_M \left(M_{\Psi'_{M_+}} \right) \right\}. \tag{A19}$$

Such situation is depicted in Figure B1, where all the surfaces discussed here are plotted in the three-population phase space $N - M - P$.

B.2 | Coexistence stability

For E_{NMP} we apply the Routh-Hurwitz conditions. For the trace of the Jacobian, we find

$$\text{tr}(J_{NMP}) = \frac{\xi_N(N^*)}{2K(1 + b_N N^*)} + \frac{\xi_M(M^*)}{2J(1 + b_M M^*)}, \tag{A20}$$

with

$$\xi_N(N^*) = -b_N(5r + 2c_{MN}K)(N^*)^2 + (b_N K(3r - s) - 3r - 2c_{MN}K)N^*$$
$$- 2a_N e_N K \sqrt{N^*} + K(r - s), \tag{A21}$$

$$\xi_M(M^*) = -b_M(5q + 2c_{NM}J)(M^*)^2 + (b_MJ(3q - s) - 3q - 2c_{NM}J)M^*$$
$$- 2a_Me_MJ\sqrt{M^*} + J(q - s). \tag{A22}$$

and for the determinant

$$\det(J_{NMP}) = T_1 + T_2 + T_3 + T_4 + T_5 + T_6 \tag{A23}$$

with

$$T_1 = -\left(\frac{r}{2} - \frac{3rN^*}{2K} + \frac{b_NrN^*}{1 + b_NN^*}\left(1 - \frac{N^*}{K}\right) - c_{NM}M^*\right)$$
$$\times \left(\frac{q}{2} - \frac{3qM^*}{2J} + \frac{b_MqM^*}{1 + b_MM^*}\left(1 - \frac{M^*}{J}\right) - c_{MN}N^*\right)$$
$$\times \left(s + \frac{a_Ne_N\sqrt{N^*}}{1 + b_NN^*} + \frac{a_Me_M\sqrt{M^*}}{1 + b_MM^*}\right),$$

$$T_2 = \left(\frac{1}{2} - \frac{b_NN^*}{1 + b_NN^*}\right)\left(1 - \frac{N^*}{K}\right)\frac{a_Mc_{NM}e_NrN^*\sqrt{M^*}}{1 + b_MM^*},$$

$$T_3 = \left(\frac{1}{2} - \frac{b_MM^*}{1 + b_MM^*}\right)\left(1 - \frac{M^*}{J}\right)\frac{a_Nc_{MN}e_MqM^*\sqrt{N^*}}{1 + b_NN^*},$$

$$T_4 = \left(\frac{q}{2} - \frac{3qM^*}{2J} + \frac{b_MqM^*}{1 + b_MM^*}\left(1 - \frac{M^*}{J}\right) - c_{MN}N^*\right)$$
$$\times \left(\frac{1}{2} - \frac{b_NN^*}{1 + b_NN^*}\right)\left(1 - \frac{N^*}{K}\right)\frac{a_Ne_Nr\sqrt{N^*}}{1 + b_NN^*},$$

$$T_5 = \left(\frac{r}{2} - \frac{3rN^*}{2K} + \frac{b_NrN^*}{1 + b_NN^*}\left(1 - \frac{N^*}{K}\right) - c_{NM}M^*\right)$$
$$\times \left(\frac{1}{2} - \frac{b_MM^*}{1 + b_MM^*}\right)\left(1 - \frac{M^*}{J}\right)\frac{a_Me_Mq\sqrt{M^*}}{1 + b_MM^*},$$

$$T_6 = \left(s + \frac{a_Ne_N\sqrt{N^*}}{1 + b_NN^*} + \frac{a_Me_M\sqrt{M^*}}{1 + b_MM^*}\right)c_{NM}c_{MN}N^*M^*.$$

We need also the sum of the principal minors of the Jacobian,

$$Z(J_{NMP}) = T_7 + T_8 + T_9 + T_{10} + T_{11} + T_{12},$$ (A24)

with

$$T_7 = \left(\frac{r}{2} - \frac{3rN^*}{2K} + \frac{b_N rN^*}{1 + b_N N^*} \left(1 - \frac{N^*}{K} \right) - c_{NM} M^* \right)$$
$$\times \left(\frac{q}{2} - \frac{3qM^*}{2J} + \frac{b_M qM^*}{1 + b_M M^*} \left(1 - \frac{M^*}{J} \right) - c_{MN} N^* \right),$$

$$T_8 = - \left(\frac{r}{2} - \frac{3rN^*}{2K} + \frac{b_N rN^*}{1 + b_N N^*} \left(1 - \frac{N^*}{K} \right) - c_{NM} M^* \right)$$
$$\times \left(s + \frac{a_N e_N \sqrt{N^*}}{1 + b_N N^*} + \frac{a_M e_M \sqrt{M^*}}{1 + b_M M^*} \right),$$

$$T_9 = - \left(\frac{q}{2} - \frac{3qM^*}{2J} + \frac{b_M qM^*}{1 + b_M M^*} \left(1 - \frac{M^*}{J} \right) - c_{MN} N^* \right)$$
$$\times \left(s + \frac{a_N e_N \sqrt{N^*}}{1 + b_N N^*} + \frac{a_M e_M \sqrt{M^*}}{1 + b_M M^*} \right),$$

$$T_{10} = -c_{NM} c_{MN} N^* M^*$$

$$T_{11} = \left(\frac{1}{2} - \frac{b_N N^*}{1 + b_N N^*} \right) \left(1 - \frac{N^*}{K} \right) \frac{a_N e_N r \sqrt{N^*}}{1 + b_N N^*},$$

$$T_{12} = \left(\frac{1}{2} - \frac{b_M M^*}{1 + b_M M^*} \right) \left(1 - \frac{M^*}{J} \right) \frac{a_M e_M q \sqrt{M^*}}{1 + b_M M^*}.$$

Stability is then ensured by

$$\text{tr}(J_{NMP}) > 0, \ \det(J_{NMP}) > 0, \ Z(J_{NMP}) < \frac{\det(J_{NMP})}{\text{tr}(J_{NMP})},$$ (A25)

where the first condition holds if and only if

$$\frac{\xi_N(N^*)}{2K(1 + b_N N^*)} > -\frac{\xi_M(M^*)}{2J(1 + b_M M^*)}.$$ (A26)